

(4)

DTIC FILE COPY

Resonance Enhanced Raman Studies of As-Grown and Laser-Processed HgCdTe

Prepared by

A. COMPAAN and B. AGGARWAL
The University of Toledo
Department of Physics and Astronomy
Toledo, OH 43606

R. C. BOWMAN, JR.
Chemistry and Physics Laboratory
Laboratory Operations
The Aerospace Corporation
El Segundo, CA 90245

and

D. E. COOPER
Rockwell International
Thousand Oaks, CA 91360

22 September 1989

Prepared for

SPACE SYSTEMS DIVISION
AIR FORCE SYSTEMS COMMAND
Los Angeles Air Force Base
P.O. Box 92960
Los Angeles, CA 90009-2960

APPROVED FOR PUBLIC RELEASE;
DISTRIBUTION UNLIMITED

DTIC
ELECTE
OCT 31 1989
S B D
89 10 31 218

UNCLASSIFIED

SECURITY CLASSIFICATION OF THIS PAGE

REPORT DOCUMENTATION PAGE

1a. REPORT SECURITY CLASSIFICATION Unclassified			1b. RESTRICTIVE MARKINGS		
2a. SECURITY CLASSIFICATION AUTHORITY			3. DISTRIBUTION/AVAILABILITY OF REPORT		
2b. DECLASSIFICATION/DOWNGRADING SCHEDULE			Approved for public release; distribution unlimited.		
4. PERFORMING ORGANIZATION REPORT NUMBER(S) TR-0089(4945-07)-1			5. MONITORING ORGANIZATION REPORT NUMBER(S)		
6a. NAME OF PERFORMING ORGANIZATION The Aerospace Corporation Laboratory Operations		6b. OFFICE SYMBOL (If applicable)	7a. NAME OF MONITORING ORGANIZATION Space Systems Division		
6c. ADDRESS (City, State, and ZIP Code) El Segundo, CA 90245-4691		7b. ADDRESS (City, State, and ZIP Code) Los Angeles Air Force Base Los Angeles, CA 90009-2960			
8a. NAME OF FUNDING/SPONSORING ORGANIZATION		8b. OFFICE SYMBOL (If applicable)	9. PROCUREMENT INSTRUMENT IDENTIFICATION NUMBER F04701-88-C-0089		
8c. ADDRESS (City, State, and ZIP Code)		10. SOURCE OF FUNDING NUMBERS			
		PROGRAM ELEMENT NO.	PROJECT NO.	TASK NO.	WORK UNIT ACCESSION NO.
11. TITLE (Include Security Classification) Resonance Enhanced Raman Studies of As-Grown and Laser-Processed HgCdTe					
12. PERSONAL AUTHOR(S) Compaan, A. and Aggarwal, B. (The University of Toledo); Bowman, R. C., Jr. (The Aerospace Corp.); and Cooper, D. E. (Rockwell International)					
13a. TYPE OF REPORT		13b. TIME COVERED FROM _____ TO _____		14. DATE OF REPORT (Year, Month, Day) 1989 September 22	
15. PAGE COUNT 20					
16. SUPPLEMENTARY NOTATION					
17. COSATI CODES			18. SUBJECT TERMS (Continue on reverse if necessary and identify by block number)		
FIELD	GROUP	SUB-GROUP	Alloy semiconductors		
			Infrared detector materials		
			Laser annealing of semiconductors		
19. ABSTRACT (Continue on reverse if necessary and identify by block number)					
<p>Raman spectroscopy in $\text{Hg}_{1-x}\text{Cd}_x\text{Te}$ (MCT) is a powerful, nondestructive surface probe of alloy composition and crystallinity. The frequencies and the relative amplitudes of the HgTe-like and CdTe-like phonon modes change with Cd fraction; the E_1 and $E_1 + \Delta_1$ critical points shift with x value and strongly influence the Raman spectra obtained with the green and blue lines of the argon laser. The resonance enhancement of the two LO and two TO modes and a "cluster" mode in as-grown samples of MCT are studied for x values between 0.20 and 0.31. Also studied are the changes that occur in the Raman spectra after exposure of the MCT surfaces to single pulses from a dye laser with pulse energies above the melt threshold. The Raman spectra show clear evidence of compositional changes near the surface when processing occurs in air. However, when the irradiation occurs in an ambient of ~ 20 atm of argon, the major effect is a reduction of the peak associated with a cluster mode. The results are consistent with a strong suppression of clustering after pulsed laser annealing.</p>					
20. DISTRIBUTION/AVAILABILITY OF ABSTRACT			21. ABSTRACT SECURITY CLASSIFICATION		
<input checked="" type="checkbox"/> UNCLASSIFIED/UNLIMITED <input type="checkbox"/> SAME AS RPT. <input type="checkbox"/> DTIC USERS			Unclassified		
22a. NAME OF RESPONSIBLE INDIVIDUAL			22b. TELEPHONE (Include Area Code)		22c. OFFICE SYMBOL

UNCLASSIFIED

SECURITY CLASSIFICATION OF THIS PAGE

18. SUBJECT TERMS (Continued)

Mercury cadmium telluride

Raman light scattering

Vibrational properties in solids

SECURITY CLASSIFICATION OF THIS PAGE

UNCLASSIFIED

PREFACE

The work at The Aerospace Corporation was supported by the U.S. Air Force Space Division under contract No. F04701-85-0086. Some of the work at The University of Toledo was done on samples kindly supplied by J. Ramsey of the Army Night Vision and Electro-optics Center.



Accession For	
NTIS GRA&I	<input checked="checked" type="checkbox"/>
DTIC TAB	<input type="checkbox"/>
Unannounced	<input type="checkbox"/>
Justification	
By	
Distribution/	
Availability Codes	
Dist	Avail and/or Special
A-1	

CONTENTS

PREFACE.....	1
I. INTRODUCTION.....	5
II. ELECTRON-PHONON COUPLING.....	7
III. EXPERIMENT.....	9
IV. RESONANCE ENHANCEMENT: AS-GROWN SAMPLES.....	11
V. LASER-ANNEALED SURFACES.....	15
VI. CLUSTER MODE.....	17
VII. CONCLUSION.....	21
REFERENCES.....	23

FIGURES

1. Raman Spectra Obtained from $\langle 111 \rangle$ Oriented Sample With 20.5% Cd for Three Argon Laser Lines.....	12
2. Raman Spectra from $\langle 111 \rangle$ Oriented Sample with 27% Cd.....	12
3. Intensities of the Four First-Order Raman Lines Plotted as a Function of the Exciting Laser Photon Energy for the Same $x = 0.205$ Sample as in Fig. 1.....	13
4. Intensities of the Four First-Order Raman Lines Plotted as a Function of the Exciting Laser Photon Energy for the Same $x = 0.27$ Sample as in Fig. 2.....	13
5. Raman Spectra from 20.5% Cd Sample With 496.5-nm Excitation.....	15
6. Raman Spectra from 20.5% Cd Sample Showing Effects of Pulsed Laser Annealing at 0.05 J/cm^2 in 20 atm of Argon Gas.....	18
7. Raman Spectra from 31% Cd Sample Showing Effects of Pulsed Laser Annealing at 0.05 J/cm^2 in 20 atm of Argon Gas.....	19

1. INTRODUCTION

Phonon Raman scattering is sensitive to the interatomic forces and the ion masses that determine the vibrational frequencies and, thus, the Raman shifts. By contrast, the intensities of the various Raman lines are sensitive to the details of the electronic band structure of the semiconductor. Thus Raman scattering is potentially capable of exploring both the average compositional changes as they affect the band structure and also local bonding arrangements in the solid. In mercury cadmium telluride (MCT), in addition, the visible-light penetration depth is only 10-20 nm so that Raman scattering is essentially a near-surface probe of these effects. The availability of a noncontact probe such as Raman scattering is particularly important for MCT because it has a delicate surface easily modified by abrasion, chemicals, heating (Ref. 1), and low-energy ion bombardment.

In this report, we present the results of a study of the resonance enhancement of four first-order Raman lines in $\text{Hg}_{1-x}\text{Cd}_x\text{Te}$ with Cd concentration (x values) ranging from 0.20 to 0.31. The photon energy was varied from 2.4 to 2.7 eV across the E_1 critical point in the joint density of electronic states. We find that details of the resonance enhancement vary depending on the type of phonon mode [transverse optical (TO), longitudinal optical (LO), or "cluster"]. In addition, we report for the first time, Raman studies on surfaces that have been pulsed laser annealed. We find that laser annealing produces significant changes in the Raman intensity of a line, which has been suggested earlier (Ref. 2) as arising from a "cluster" mode. (Although the association of this mode with nonstatistical clustering of the Hg and Cd has not been fully proven, we find this interpretation plausible, especially in view of the results presented here.)

Evidence from Raman (Ref. 2), infrared (Ref. 3), and nuclear magnetic resonance (Ref. 4) studies of MCT has recently indicated that clustering may be occurring in which nearest-neighbor bonding arrangements are not distributed with statistical probabilities. $\text{Hg}_{1-x}\text{Cd}_x\text{Te}$ is a ternary alloy semiconductor with the common anion Te. In MCT, as well as several other alloy semiconductors, there has been considerable interest recently in the specific cation arrangements that may arise during growth. It has been suggested that ordered growth may occur in which each anion is surrounded by

the same arrangement of cations (Ref. 5). For tetrahedrally bonded semiconductors, such completely ordered growth is normally only possible when the cation ratios are either 1:3, 2:2, or 3:1. For other ratios, there may nevertheless be a preferential clustering of cations in these ratios. That is, the number of anions with nearest neighbors in these ratios may be much larger than that predicted by a statistical distribution (Ref. 6).

Alloy ordering can improve carrier mobility by reducing scattering due to alloy disorder and by eliminating carrier localization due to localized fluctuations in the band gap. This could affect the performance of IR detectors fabricated in MCT, since the detector response depends on minority carrier diffusion into junction regions.

The use of nanosecond pulsed laser annealing provides access to an extremely rapid method of crystallizing the semiconductor. Cooling rates exceeding 10^9 K/sec are readily achieved (Ref. 7). This is radically different from the near-equilibrium growth conditions present during liquid-phase epitaxial growth, Bridgeman growth, or Czochralski growth. It is plausible to expect that if the formation of clusters has a slight energetic advantage, clustering may occur in near-equilibrium growth but would be greatly suppressed during the rapid quench that occurs during the pulsed laser annealing process. We believe that the data presented here provide preliminary evidence that these effects are indeed occurring.

II. ELECTRON-PHONON COUPLING

For the polar II-VI semiconductors, the electron-phonon coupling mechanism that is responsible for the Raman strength of the transverse optical (TO) mode is the deformation potential, which depends on short-range interactions. However, Raman scattering of the longitudinal optical (LO) phonon modes can be produced both by the deformation potential and by the long-range electric field of the LO phonon (Ref. 8). This is known as Fröhlich coupling. Under near-resonance conditions, the Fröhlich coupling nearly always dominates the deformation potential for LO scattering in polar semiconductors.

Menendez et al. (Ref. 8) have recently studied the resonance Raman behavior of the LO and 2 LO peaks for this alloy system with $x \sim 1$ in a geometry in which the LO is forbidden. We report here the first systematic study of the resonance behavior of both the TO and LO modes for Cd fraction in the range from 0.20 to 0.31. We have chosen to compare the behavior of the LO with that of the TO mode because of the difference in mechanisms (short vs long range interactions) and their possible sensitivity to clustering in these alloys.

III. EXPERIMENT

Raman scattering was performed at liquid nitrogen temperature on a variety of bulk and liquid phase epitaxial (LPE) samples with x values of 0.205, 0.23, 0.27, and 0.31. Of these compositions, the last two were bulk crystals, and Raman scattering was obtained from the $\langle 100 \rangle$, $\langle 110 \rangle$, and $\langle 111 \rangle$ faces. The other samples had been grown by LPE and therefore were available only with $\langle 111 \rangle$ surfaces. Only the LO modes are observable from the $\langle 100 \rangle$ face, only the TO modes are seen from the $\langle 110 \rangle$ face, but both LO and TO modes are allowed from the $\langle 111 \rangle$ face. The laser beam was focused by a cylindrical lens to form an extended line image on the sample in order to avoid laser heating and surface decomposition. Power density at the sample was typically less than 50 W/cm^2 , with a total power of no more than 140 mW.

The laser annealing was performed with a Nd:YAG-pumped dye laser operating at 728 nm with a pulse duration of ~ 8 nsec. The dye laser was chosen because of its smoother beam profile than the frequency-doubled YAG and broader bandwidth which helps to minimize laser speckle problems. The dye laser beam was weakly focused with a 1.5-m focal length lens. Initial annealing experiments were done in air ambients, and strong deterioration of the surface occurred--evidence of metallic tellurium appeared in the Raman spectra. All further annealing was done in an inert atmosphere. We found that excellent results could be obtained with the samples held in a pressurized cell under ~ 20 atm of argon pressure.

Transient reflectivity measurements indicated that the melting threshold in air is approximately 0.02 J/cm^2 . Annealing was performed at this energy and also at 0.05 J/cm^2 and 0.14 J/cm^2 . Some decomposition was observed at the highest pulse energy, and thus most results reported here are from single-pulse anneals at 0.05 J/cm^2 . The beam cross section at the sample was typically $0.5 \text{ mm} \times 0.08 \text{ mm}$. Some results were obtained with the sample rastered along the long dimension of the spot with the sample translated by 0.5 mm between pulses.

IV. RESONANCE ENHANCEMENT: AS-GROWN SAMPLES

For $\text{Hg}_{1-x}\text{Cd}_x\text{Te}$ with x values from 0.20 to 0.31, the fundamental gap E_0 ranges from ~ 0.1 to 0.3 eV at liquid helium temperature. The second direct gap E_1 lies in the middle of the visible range, 2.4 to 2.5 eV (Ref. 9). This E_1 critical point in the joint density of electronic states is responsible for most of the strength of the phonon Raman scattering when observed with the green and blue lines of the argon laser. Thus, a strong resonance enhancement occurs as the exciting frequency is tuned through the E_1 gap (Ref. 9).

The resonance enhancement affects the various peaks in the Raman spectrum in different ways, as the spectra in Fig. 1 illustrate for a sample with $x = 20.5\%$. Note that the intensity of the TO_2 mode at 120 cm^{-1} is quite constant over the range from 514.5 nm (2.4 eV) to 476.5 nm (2.6 eV). However, the intensity of the "cluster" mode at 133 cm^{-1} and that of the LO modes at 140 cm^{-1} and 157 cm^{-1} are decreasing rapidly over this same spectral region.

Similar differences among the enhancements of the various modes are observed for samples of other compositions. Figure 2 illustrates the behavior for a sample with $x = 27\%$. Here the changes are even more striking. The "cluster" mode dominates the spectrum for 514.5 nm , but for 476.5 nm the TO_2 mode dominates.

The resonance enhancements of the intensities of the four modes are summarized in Figs. 3 and 4 in which the line intensities are displayed as a function of the photon energy of the exciting laser. Between 20.5% Cd (Fig. 3) and 27% (Fig. 4), the position of the E_1 gap moves higher by about 50 meV and the position of the maximum intensity of the three higher-frequency Raman lines similarly moves to higher energy. The maximum intensity for these three lines corresponds closely to the position of the E_1 critical point. For the TO_2 mode at $\sim 120\text{ cm}^{-1}$, however, it appears that the resonance behaves like a step function, increasing rapidly at the E_1 energy and remaining high above E_1 .

Note that the data shown in Figs. 3 and 4 have not been corrected for the effects of the spectrometer throughput (minor) and also have not been adjusted for the effects of the changing penetration depth of the laser light (significant) and other effects related to the changing optical constants (Ref. 10).

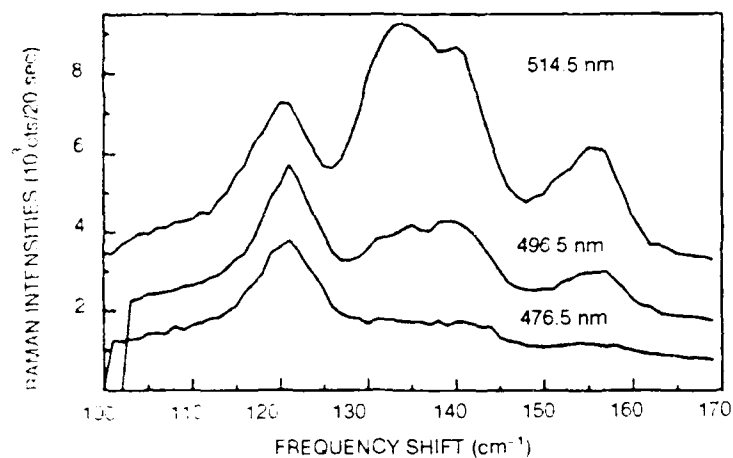


Fig. 1. Raman Spectra Obtained from $\langle 111 \rangle$ Oriented Sample with 20.5% Cd for Three Argon Laser Lines. Note that the middle and upper traces have been shifted up by 1000 and 2000 counts, respectively.

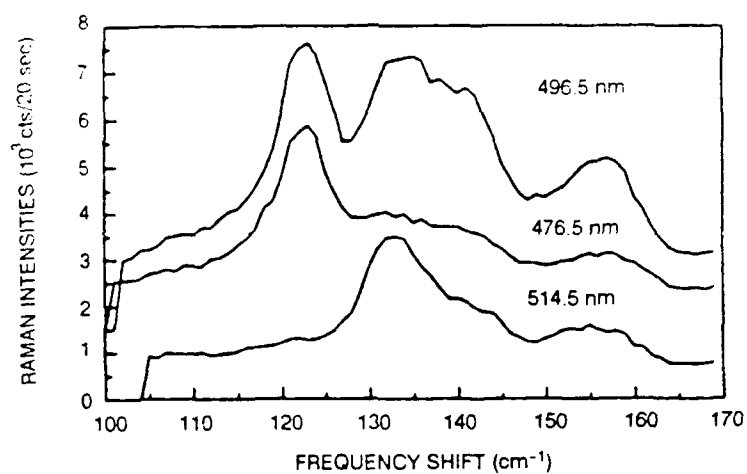


Fig. 2. Raman Spectra from $\langle 111 \rangle$ Oriented Sample with 27% Cd. Top two traces are shifted up by 1500 counts.

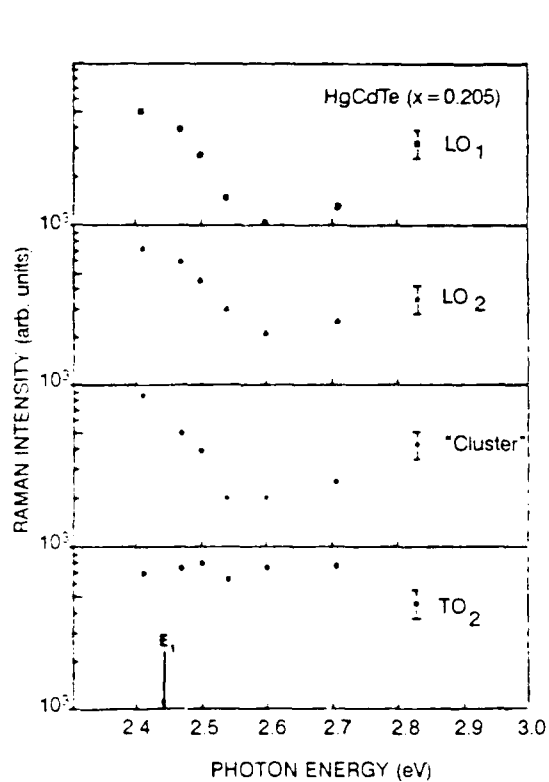


Fig. 3. Intensities of the Four First-Order Raman Lines Plotted as a Function of the Exciting Laser Photon Energy for the Same $x = 0.205$ Sample as in Fig. 1.

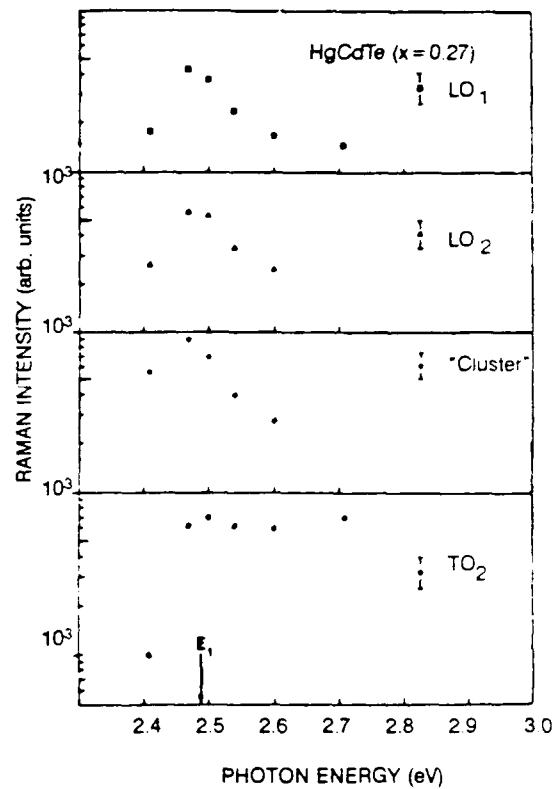


Fig. 4. Intensities of the Four First-Order Raman Lines Plotted as a Function of the Exciting Laser Photon Energy for the Same $x = 0.27$ Sample as in Fig. 2.

V. LASER-ANNEALED SURFACES

With a laser pulse energy of 0.05 J/cm^2 , the surface temperature of the MCT rises rapidly to the melting point and remains there for a period of 100 to 200 nsec. During this time the high vapor pressure of the constituents can lead to surface deterioration and loss of stoichiometry. Evidence of this was found by Raman scattering on samples that were laser-annealed in air ambients. Figure 5 illustrates these effects. The spectra from the air-annealed surface show strong peaks from pure polycrystalline Te (Ref. 11) at 127 cm^{-1} and 142 cm^{-1} . These peaks completely dominate the spectra on these samples.

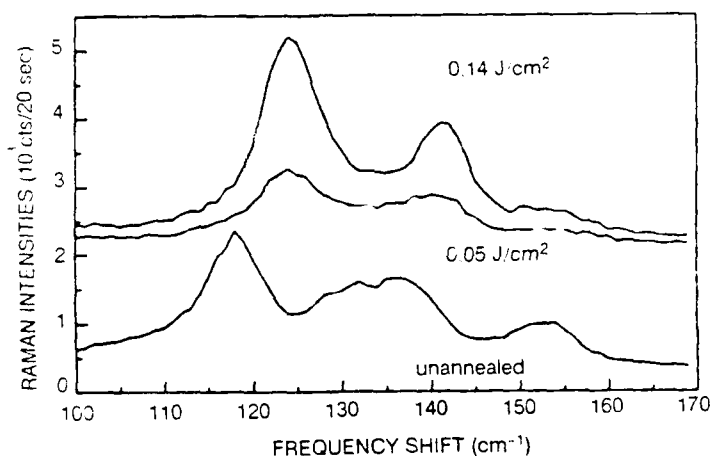


Fig. 5. Raman Spectra from 20.5% Cd Sample with 496.5-nm Excitation. Top two traces shifted by +2000 counts. Annealing performed in air with 8-nsec dye laser ($\lambda = 728 \text{ nm}$).

To avoid this surface deterioration, the same samples were also laser annealed in argon gas ambients. (It was possible to treat each surface with several different pulse anneals since each laser pulse affected approximately a 1-mm-diameter spot.) In an argon ambient of 1 atm, much less decomposition of the surface occurred. Increasing the argon pressure to 20 atm (Ref. 12) produced no noticeable deterioration at power densities below $\sim 0.10 \text{ J/cm}^2$. The overpressure of argon appears to be quite effective at slowing the outdiffusion of Hg and Cd away from the molten surface and thus protecting the surface stoichiometry. The Raman spectra give no evidence of compositional changes until power densities of $\sim 0.14 \text{ J/cm}^2$. Several samples were therefore annealed at 0.5 J/cm^2 in the 20-bar argon ambient.

VI. CLUSTER MODE

The most significant change that occurs in the Raman spectra from the laser-annealed spots is that the intensity of the cluster mode is greatly reduced for all exciting lines of the laser. Comparison spectra before and after annealing are shown in Fig. 6 for laser wavelengths of 514.5 and 496.5 nm for the 20% sample.

Amirtharaj et al. (Ref. 2) have interpreted this mode as arising from nonrandom "clustering" of the Cd and Hg atoms in a way similar to that discussed by Verleur and Barker (Ref. 6) for the case of the alloy GaAsP. Lattice dynamics calculations by Fu and Dow (Ref. 13) have indicated that this peak would arise from Te surrounded by 3 Hg and 1 Cd. (However, the calculations showed that nonstoichiometric clustering was not needed for this mode to appear prominently in the phonon density of states.)

Figure 7 illustrates the effects of pulsed laser annealing on the <111> sample with 31% Cd. Again, the strongest effect is the reduction of the cluster mode. There also appears to be some narrowing of the Raman peaks after the laser anneal.

Additional measurements are needed to confirm the origin of the laser-annealing-induced changes in the Raman spectra; however, one possible interpretation is that the rapid quench which occurs during the laser anneal produces changes in the local stoichiometry. If nonrandom arrangements of the cations do occur during normal near-equilibrium growth, then the rapid quench from temperatures well above the melting temperature are likely to freeze atoms in arrangements that are more nearly random. It should be noted that recent ^{125}Te nuclear magnetic resonance (NMR) measurements (Ref. 4) obtained on bulk samples do indicate that there is a substantial excess of Te environments with 3 Hg and 1 Cd in this range of x values above that predicted by a statistical distribution (Bernoulli polynomial).

In $\text{Hg}_{1-x}\text{Cd}_x\text{Te}$ with $x = 0.31$, a maximum of 92% of the Te sites can possess a single Cd neighbor, whereas the random statistical probability of this configuration is 41%. Laser annealing reduces the intensity of the cluster mode scattering by a factor of approximately 2, which is consistent with a transition from nearly maximum clustering to a random distribution.

It is also possible that some change of large-scale surface stoichiometry could produce the observed changes in the Raman spectra, even though the other phonon peaks show no clear evidence of shifts in the resonant Raman peaks. Hg diffusion of HgMnTe has been observed with cw CO₂ laser annealing (Ref. 14), but in that case the time scales are much longer and the samples do not make a transition through the melt phase.

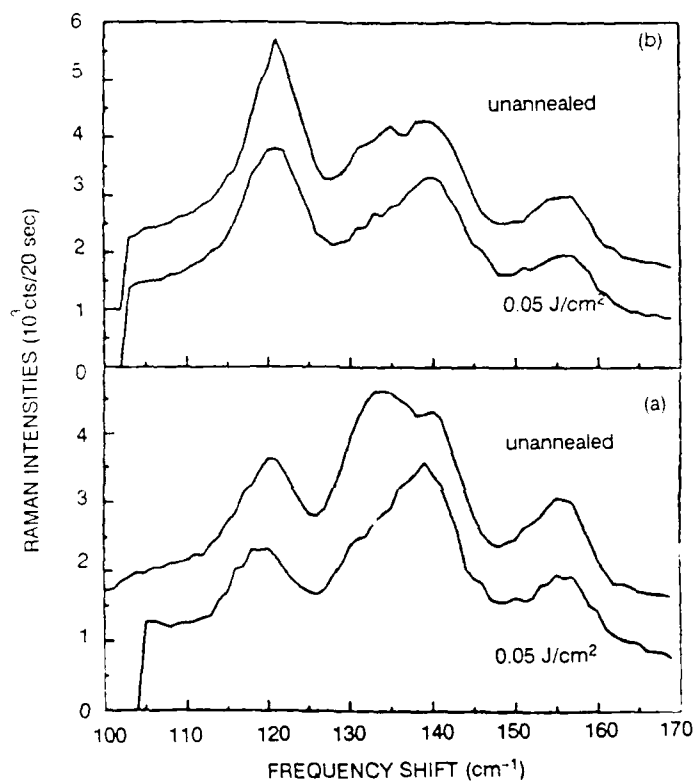


Fig. 6. Raman Spectra from 20.5% Cd Sample Showing Effects of Pulsed Laser Annealing at 0.05 J/cm² in 20 atm of Argon Gas. 20.5% Cd sample with <111> surface. (a) $\lambda = 514.5$ nm, (b) $\lambda = 496.5$ nm. Top traces shifted +1000 counts.

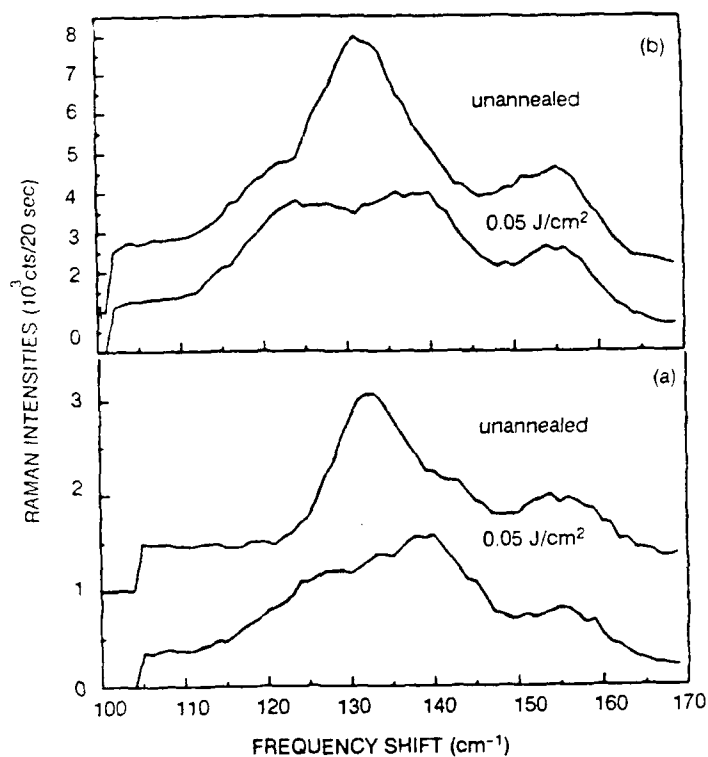


Fig. 7. Raman Spectra from 31% Cd Sample Showing Effects of Pulsed Laser Annealing at 0.05 J/cm^2 in 20 atm of Argon Gas. 31% Cd sample with $\langle 111 \rangle$ surface. (a) $\lambda = 514.5 \text{ nm}$, (b) $\lambda = 496.5 \text{ nm}$. Top traces shifted +1000 counts.

VII. CONCLUSION

The resonance enhancement of the intensities of four lines in the Raman spectra of $\text{Hg}_{1-x}\text{Cd}_x\text{Te}$ has been studied. We find that the enhancement of the HgTe-like TO_2 mode undergoes a sharp rise at the E_1 band edge and then remains high. By contrast, the enhancements of the HgTe-like LO_2 mode, the "cluster" mode, and the CdTe-like modes undergo a strong maximum very near the position of the E_1 gap. The difference in resonance behavior is probably related to the different nature of the electron-phonon coupling: short-range for the TO and long-range for the LO mode.

Raman scattering from pulsed-annealed surfaces of these samples indicates that the cluster mode is strongly suppressed following the anneal. It is reasonable to expect that this is a natural consequence of the rapid quench from melting temperatures which occurs during the pulsed laser anneal process. More generally, it may be anticipated that growth processes far from equilibrium, such as pulsed laser annealing and molecular beam epitaxy, might suppress the tendency toward clustering which may occur during near-equilibrium growth processes.

REFERENCES

1. D. E. Aspnes and H. Arwin, J. Vac. Sci. Technol. A **2**, 1309 (1984); H. Arwin and D. E. Aspnes, J. Vac. Sci. Technol. A, **2**, 1316 (1984).
2. P. M. Amirtharaj, K. K. Tiong, P. Parayanthal, F. H. Pollak, and J. K. Furdyna, J. Vac. Sci. Technol. A **3**, 226 (1985).
3. L. K. Vodopyanov, S. P. Kozyrev, Yu. A. Aleschenko, R. Triboulet, and Y. Marfaing, Proc. 17th Int. Conf. Phys. of Semiconductors, 1984, p. 947.
4. D. Azmir, K. Beshah, P. Becla, P. A. Wolff, R. G. Griffin, D. Zax, S. Vega, and N. Yellin, J. Vac. Sci. Technol. A **6**, 2612 (1988).
5. See for example, J. E. Bernard, S.-H. Wei, D. M. Wood, and A. Zunger, Appl. Phys. Lett. **52**, 311 (1988); A. Gomyo, T. Suzuki, and S. Iijima, Phys. Rev. Lett. **60**, 2645 (1988); T. S. Kuan, W. I. Wang, and E. L. Wilkie, Appl. Phys. Lett. **51**, (1987).
6. H. W. Verleur and A. S. Barker, Phys. Rev. **149**, 715 (1966).
7. A. Lietoila and J. F. Gibbons, J. Appl. Phys. **53**, 3207 (1982); A. Compaan, M. C. Lee, and G. J. Trott, Phys. Rev. B **32**, 6731 (1985).
8. J. Menendez, M. Cardona, and L. K. Vodopyanov, Phys. Rev. B, **31**, 3705 (1985).
9. Landoldt-Bornstein, Numerical Data and Functional Relationships in Science and Technology, Vol. 17c (Physics of Group II-VI Semiconductors and Alloys) (Springer, Berlin, 1982).
10. A. Compaan and H. J. Trodanl, Phys. Rev. B **29**, 793 (1984).
11. P. M. Amirtharaj and F. H. Pollak, Appl. Phys. Lett. **45**, 789 (1984).
12. B. Aggarwal and A. Compaan, Bull. Am. Phys. Soc. **33**, 809 (1988).
13. Z-W. Fu and J. D. Dow, Phys. Rev. B **36**, 7625 (1987).
14. F. G. Moore and R. E. Kremer, Appl. Phys. Lett. **52**, 1314 (1988).

LABORATORY OPERATIONS

The Aerospace Corporation functions as an "architect-engineer" for national security projects, specializing in advanced military space systems. Providing research support, the corporation's Laboratory Operations conducts experimental and theoretical investigations that focus on the application of scientific and technical advances to such systems. Vital to the success of these investigations is the technical staff's wide-ranging expertise and its ability to stay current with new developments. This expertise is enhanced by a research program aimed at dealing with the many problems associated with rapidly evolving space systems. Contributing their capabilities to the research effort are these individual laboratories:

Aerophysics Laboratory: Launch vehicle and reentry fluid mechanics, heat transfer and flight dynamics; chemical and electric propulsion, propellant chemistry, chemical dynamics, environmental chemistry, trace detection; spacecraft structural mechanics, contamination, thermal and structural control; high temperature thermomechanics, gas kinetics and radiation; cw and pulsed chemical and excimer laser development including chemical kinetics, spectroscopy, optical resonators, beam control, atmospheric propagation, laser effects and countermeasures.

Chemistry and Physics Laboratory: Atmospheric chemical reactions, atmospheric optics, light scattering, state-specific chemical reactions and radiative signatures of missile plumes, sensor out-of-field-of-view rejection, applied laser spectroscopy, laser chemistry, laser optoelectronics, solar cell physics, battery electrochemistry, space vacuum and radiation effects on materials, lubrication and surface phenomena, thermionic emission, photo-sensitive materials and detectors, atomic frequency standards, and environmental chemistry.

Computer Science Laboratory: Program verification, program translation, performance-sensitive system design, distributed architectures for spaceborne computers, fault-tolerant computer systems, artificial intelligence, micro-electronics applications, communication protocols, and computer security.

Electronics Research Laboratory: Microelectronics, solid-state device physics, compound semiconductors, radiation hardening; electro-optics, quantum electronics, solid-state lasers, optical propagation and communications; microwave semiconductor devices, microwave/millimeter wave measurements, diagnostics and radiometry, microwave/millimeter wave thermionic devices; atomic time and frequency standards; antennas, rf systems, electromagnetic propagation phenomena, space communication systems.

Materials Sciences Laboratory: Development of new materials: metals, alloys, ceramics, polymers and their composites, and new forms of carbon; non-destructive evaluation, component failure analysis and reliability; fracture mechanics and stress corrosion; analysis and evaluation of materials at cryogenic and elevated temperatures as well as in space and enemy-induced environments.

Space Sciences Laboratory: Magnetospheric, auroral and cosmic ray physics, wave-particle interactions; magnetospheric plasma waves; atmospheric and ionospheric physics; density and composition of the upper atmosphere, remote sensing using atmospheric radiation; solar physics, infrared astronomy, infrared signature analysis; effects of solar activity, magnetic storms and nuclear explosions on the earth's atmosphere, ionosphere and magnetosphere; effects of electromagnetic and particulate radiations on space systems; space instrumentation.